Eur. Phys. J. A **31**, 560–565 (2007)
DOI 10.1140/epja/i2006-10239-9

THE EUROPEAN PHYSICAL JOURNAL A

Special Article – QNP 2006

Nucleon elastic form factors

Current status of the experimental effort

D. Day[a]

Department of Physics, University of Virginia, Charlottesville, VA 22904, USA

Received: 8 November 2006
Published online: 6 March 2007 –

Abstract. The nucleon form factors are still the subject of active investigation even after an experimental effort spanning 50 years. This is because they are of critical importance to our understanding of the electromagnetic properties of nuclei and provide a unique testing ground for QCD motivated models of nucleon structure. Progress in polarized beams, polarized targets and recoil polarimetry have allowed an important and precise set of data to be collected over the last decade. I will review the experimental status of elastic electron scattering from the nucleon along with an outlook for future progress.

PACS. 14.20.Dh Protons and neutrons – 13.40.Gp Electromagnetic form factors – 24.70.+s Polarization phenomena in reactions

1 Introduction

The experimental and theoretical study of the nucleon elastic form factors that began more than 50 years ago has returned to an examination of its roots —the Rosenbluth formula and the validity of one-photon approximation on which it depends. Deviations from this approximation are being examined to understand how they might alter our analysis of past, current and future electron scattering data. The Rosenbluth formula, which describes the elastic electro-nucleon cross-section in terms of the Pauli and Dirac form factors and is valid only in the one-photon approximation, had been considered unassailable until the appearance of high-Q^2 polarization transfer data on the proton from Jefferson Lab.

In the single-photon exchange, the Rosenbluth formula for the elastic cross-section is written (with F_1 and F_2 the Dirac and Pauli form factors, respectively, and which are functions of momentum transfer, $Q^2 = 4E_0E'\sin^2(\theta/2)$ alone) as

$$\frac{\mathrm{d}\sigma}{\mathrm{d}\Omega} = \sigma_{\mathrm{Mott}}\frac{E'}{E_0}\left\{(F_1)^2 + \tau\left[2\left(F_1+F_2\right)^2\tan^2(\theta) + (F_2)^2\right]\right\}, \quad (1)$$

where $\tau = \frac{Q^2}{4M^2}$, θ is the electron scattering angle, E_0, E' are the incident and final electron energies, respectively, and σ_{Mott} is the Mott cross-section. Because of their direct relation (in the Breit frame) to the Fourier transforms of the charge and magnetization distributions in the nucleon, the Sachs form factors are commonly used. They are linear combinations of F_1 and F_2: $G_E = F_1 - \tau F_2$ and $G_M = F_1 + F_2$. Early measurements of the form factors established a scaling law relating three of the four nucleon elastic form factors and the dipole law describing their common Q^2-dependence, $G_E^p(Q^2) \approx \frac{G_M^p(Q^2)}{\mu_p} \approx \frac{G_M^n(Q^2)}{\mu_n} \approx G_D \equiv \left(1 + Q^2/0.71\right)^{-2}$. This behavior is known as form factor scaling. The neutron electric form factor has been usefully parametrized by $G_E^n = -\mu_N G_D \frac{\tau}{1+5.6\tau}$ [1].

2 Proton form factors

The proton form factors have been, until recently, only separated through the Rosenbluth technique, which can be understood by re-writing eq. (1) using the Sachs form factors,

$$\frac{\mathrm{d}\sigma}{\mathrm{d}\Omega} = \sigma_{\mathrm{NS}}\left[\frac{G_E^2 + \tau G_M^2}{1+\tau} + 2\tau G_M^2\tan^2(\theta/2)\right], \quad (2)$$

and rearranging, with $\epsilon^{-1} = 1 + 2(1+\tau)\tan^2(\theta/2)$ and $\sigma_{\mathrm{NS}} = \sigma_{\mathrm{Mott}}E'/E_0$, to give

$$\sigma_{\mathrm{R}} \equiv \frac{\mathrm{d}\sigma}{\mathrm{d}\Omega}\frac{\epsilon(1+\tau)}{\sigma_{\mathrm{NS}}} = \tau G_M^2(Q^2) + \epsilon G_E^2(Q^2). \quad (3)$$

By making measurements at a fixed Q^2 and variable $\epsilon(\theta, E_0)$, the reduced cross-section σ_{R} can be fit with a straight line with slope G_E^2 and intercept τG_M^2. Figure 1 gives an example of the reduced cross-section plotted in this way. The Rosenbluth formula holds only for single-photon exchange and it has been assumed (until recently) that any two-photon contribution is small.

[a] e-mail: dbd@virginia.edu

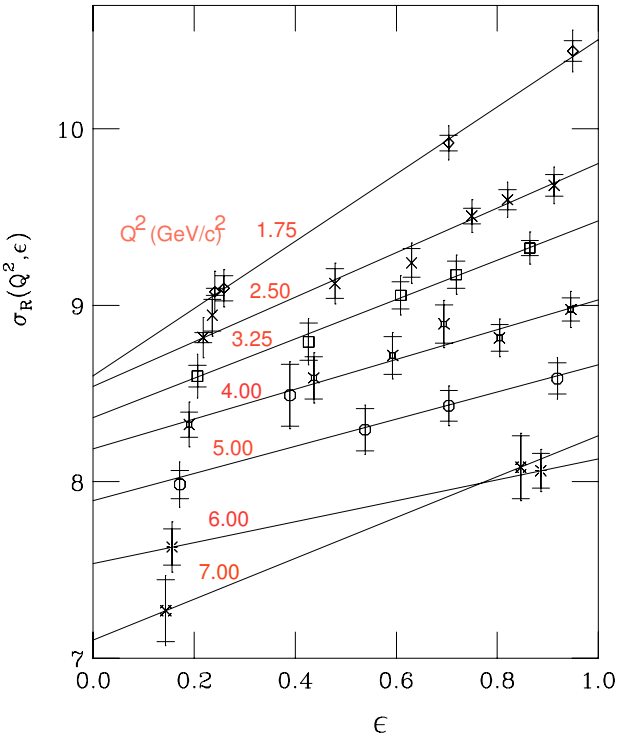

Fig. 1. Reduced cross-section plotted against ϵ for a range of fixed momentum transfers. The data is fit with a straight line with a slope G_E^2 and an intercept τG_M^2. The linear dependence of the reduced cross-section on ϵ assumes that any two-photon exchange effects are small. The data is from ref. [2].

The Rosenbluth method is problematic —it requires the measurement of absolute cross-sections and at large Q^2 the cross-section is insensitive to G_E and the error propagation is not favorable. Figure 2 presents the Rosenbluth data set. See ref. [3] for a compilation of the data, references, and useful fits. G_M^p has been successfully measured out to 30 (GeV/c)^2, while G_E^p begins to endure large errors at much smaller Q^2.

2.1 Neutron form factors

The neutron form factor data set (setting aside recent progress) has been inadequate in both quality and extent due to the lack of a free neutron target and the dominance of G_M^n over G_E^n. The traditional techniques (restricted to the use of unpolarized beams and targets) used to extract information about G_M^n and G_E^n have been: elastic scattering from the deuteron (D): $D(e,e')D$; inclusive quasielastic scattering: $D(e,e')X$; scattering from deuteron with the coincident detection of the scattered electron and recoiling neutron: $D(e,e'n)p$; a ratio method which minimizes uncertainties in the deuteron wave function and the role of FSI: $\frac{D(e,e'n)}{D(e,e'p)}$. The G_M^n data is shown in fig. 3. New data at large momentum transfers is available from an experiment [4–6] at Jefferson Lab, which used the ratio method to measure G_M^n with small errors out to nearly 5 (GeV/c)^2 in the CLAS.

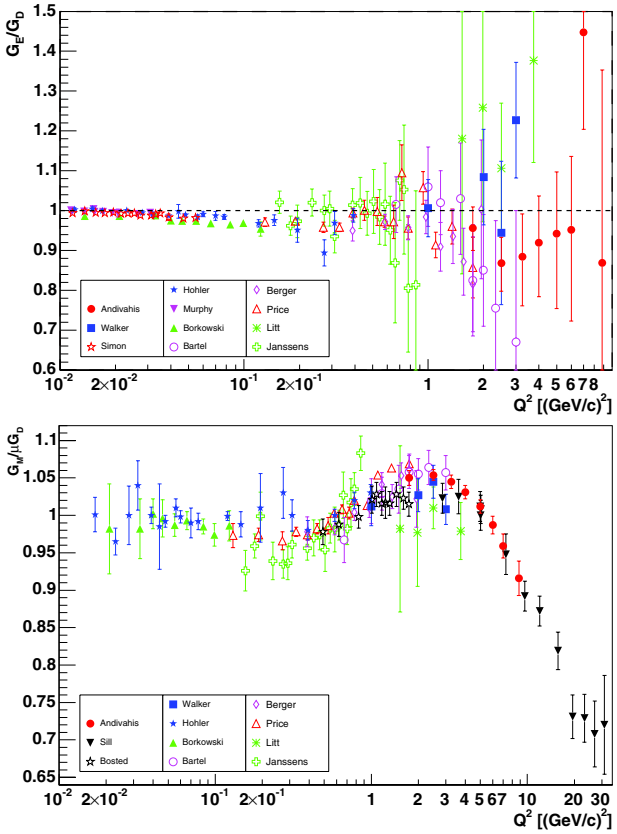

Fig. 2. G_E^p/G_D and $G_M^p/\mu_p/G_D$ *versus* Q^2 from the Rosenbluth method. The scaling law and the dipole law hold to a good approximation ($\approx 10\%$) for both form factors out to $Q^2 = 8$ (GeV/c)^2.

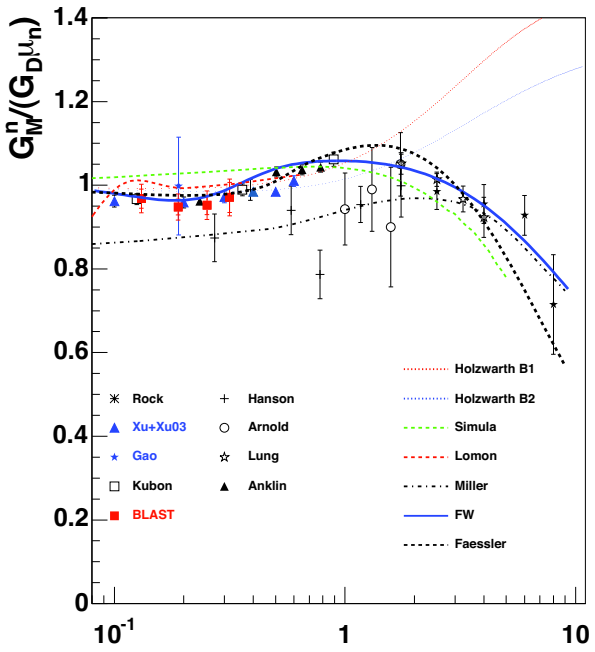

Fig. 3. G_M^n from unpolarized scattering [7–12] and polarized scattering [13–15] along with some theoretical predictions.

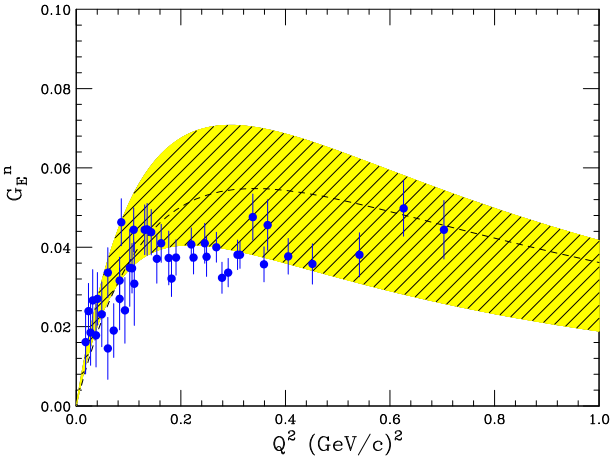

Fig. 4. G_E^n from elastic e-D [16]. The band represents the theoretical error associated with the extraction. The dashed line is the familiar Galster parametrization [1].

Until the early 1990s the extraction of G_E^n was done most successfully through either small-angle elastic e-D scattering [1,16] or by quasielastic e-D scattering [7]. In the Impulse Approximation (IA) the elastic electron-deuteron cross-section is the sum of proton and neutron responses with deuteron wave function weighting.

Experiments have been able to achieve small statistical errors but remain very sensitive to deuteron wave function model leaving a significant residual dependence on the NN potential. The most precise data on G_E^n from elastic e-D scattering are shown in fig. 4 from an experiment at Saclay, published in 1990 [16]. The band, a measure of the theoretical uncertainty, arises from the use of different NN potentials in the extraction.

3 Spin-dependent measurements

The nucleon electromagnetic form factors can be measured through spin-dependent elastic scattering from the nucleon, accomplished either through a measurement of the scattering asymmetry of polarized electrons from a polarized nucleon target [17,18] or equivalently by measuring the polarization transferred to the nucleon [19,20]. In the scattering of polarized electrons from a polarized target, an asymmetry appears in the elastic scattering cross-section when the beam helicity is reversed. In contrast, in scattering a polarized electron from an unpolarized target, the transferred polarization to the nucleon produces an azimuthal asymmetry in the secondary scattering of the nucleon (in a polarimeter) due to its dependence on the polarization. In both cases, the asymmetry is sensitive to the product $G_E G_M$. In the last decade experiments exploiting these spin degrees of freedom have become possible.

Extraction of the neutron form factors (necessarily from a nuclear target) using polarization observables is complicated by the need to account for Fermi motion, MEC, and FSI, complications that are absent when scattering from a proton target. Fortunately, it has been found for the deuteron that in kinematics that emphasize quasifree neutron knockout both the transfer polarization P_t [21] and the beam-target asymmetry A_V^{eD} [22] are especially sensitive to G_E^n and relatively insensitive to the NN potential describing the ground state of the deuteron and other reaction details. Calculations [23] of the beam-target asymmetry from a polarized ^{3}He target (which can be approximated as a polarized neutron) showed modest model dependence.

3.1 Recoil polarization

In elastic scattering of polarized electrons from a nucleon, the nucleon obtains (is transferred) a polarization whose components, P_l (along the direction of the nucleon momentum) and P_t (perpendicular to the nucleon momentum) are proportional to G_M^2 and $G_E G_M$, respectively. The recoil polarization technique has allowed precision measurements of G_E^p to nearly 6 (GeV/c)^2 [24–26] and of G_E^n out to $Q^2 = 1.5$ (GeV/c)^2 [27–30]. Polarimeters are sensitive only to the perpendicular polarization components so precession of the nucleon spin before the polarimeter in the magnetic field of the spectrometer (for the proton) or a dipole (inserted in the path of neutron) allows a measurement of the ratio P_t/P_l and the form factor ratio: $\frac{G_E}{G_M} = -\frac{P_t}{P_l}\frac{(E_0+E')}{2M_N}\tan(\theta/2)$.

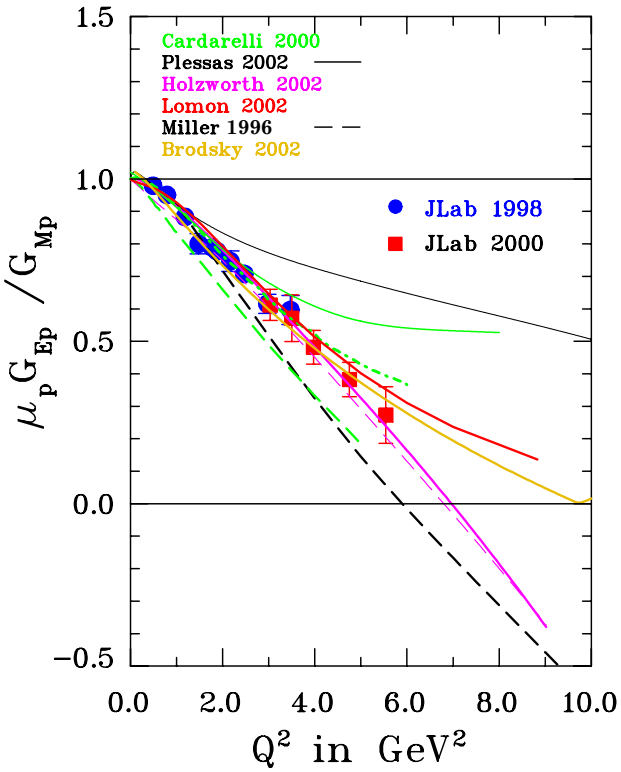

Fig. 5. (Color online) Comparison of theoretical model calculations with the data from ref. [24] (solid circles) and from [26] (solid squares). The curves are, black thin solid [31], green solid, dot-dashed and dashed [32], black dashed [33], red solid [34], yellow solid [35] and magenta dashed and solid [36].

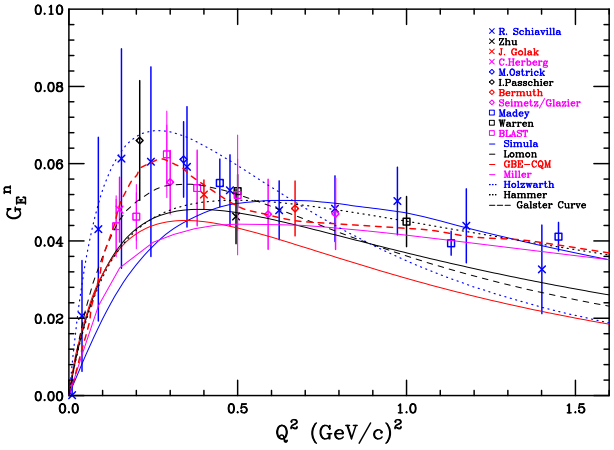

Fig. 6. (Color online) Comparison of selected theoretical model calculations with the data on G_E^n from polarized experiments. Starting at the top of the legend the data are from [37–39,28,29,40–42,30,43,44]. The neutron, at large momentum transfers, has the same Q^2-dependence as the proton. The red dashed line is the Friedrich and Walcher [45] fit to the data.

The results from Jefferson Lab for the proton are shown in fig. 5 where it is seen that the ratio of $\mu_p G_E^p/G_M^p$ does not follow the scaling law obtained from Rosenbluth separation, rather showing a steep decline with increasing Q^2. This suggests that the distribution of magnetization and charge densities in the proton are dissimilar. Shown with the data are a collection of calculations including several relativistic constituent-quark models (rQCM), a VMD-pQCD model and a chiral soliton model. Also shown is a pQCD calculation [35]. The same data, in terms of Q^2F_2/F_1, gives no indication of scaling at high momentum transfer, in contradiction to the early pQCD prediction [46]. Recent efforts [35], still within pQCD and including higher twist contributions, have been able to reproduce this behavior. Other pQCD calculations which consider quark angular orbital momentum are also successful [47,48]. For a discussion of the theoretical curves see ref. [49].

Recoil polarization has been used at both Jefferson Lab and Mainz to extract G_E^n/G_M^n when scattering polarized electrons from an unpolarized deuteron target in quasielastic kinematics. At both labs a dipole magnet was used to precess the neutron spin thereby allowing a measurement of both polarization components. The results from [30] are especially precise, extending our knowledge of G_E^n out to 1.5 GeV/c^2. See fig. 6.

3.2 Beam-target asymmetry

Polarized targets have been used to extract G_E^n [50,40,51,41,42,39,38,43] and G_M^n [52,13–15]. The beam-target asymmetry can be written schematically (a, b, c, and d are known kinematic factors) as

$$A = \frac{a\cos\Theta^\star \left(G_M\right)^2 + b\sin\Theta^\star\cos\Phi^\star G_E G_M}{c\left(G_M\right)^2 + d\left(G_E\right)^2} \qquad (4)$$

where $\Theta^\star$ and $\Phi^\star$ fix the target polarization axis. With the target polarization axis in the scattering plane and perpendicular to $\boldsymbol{q}$, $(\Theta^\star, \Phi^\star = 90°, 0°)$ the asymmetry A_{TL} is proportional to $G_E G_M$. With the polarization axis in the scattering plane and parallel to $\boldsymbol{q}$ $(\Theta^\star, \Phi^\star = 0°, 0°)$, measuring the asymmetry A_T allows G_M to be determined. See fig. 3.

G_E^n has been extracted from beam-target asymmetry measurements using polarized ^{3}He targets at Mainz and polarized ND_3 targets at Jefferson Lab, and polarized gas targets at NIKHEF and Bates. Data for G_E^n from both kinds of double-polarization experiments are shown in fig. 6 along with some relevant calculations. The models, starting with the first in the legend, include a rCQM [53], a hybrid VMD-pQCD model [34], a relativistic CQM calculation [31], a light-front cloudy bag model [54], a soliton model [36], and a dispersion theory calculation [55]. While most of these calculations describe the Q^2-dependence, several badly fail to reproduce the slope at $Q^2 = 0$, $\frac{\mathrm{d}G_E^n(0)}{\mathrm{d}Q^2} = -\frac{1}{6}\left\langle r_E^2\right\rangle$. The neutron charge radius, r_E, has been determined through neutron electron scattering [56].

4 Pion cloud

The neutron has long been thought to exist, part of the time, as a proton core surrounded by a negative pion cloud. This idea has appeared in models describing the nucleon form factors, ref. [57] and ref. [58], and has been recently re-emphasized by Friedrich and Walcher [45]. These authors fit all form factors consistently as a sum of a broad distribution and a "bump", where the "bump" is attributed to a π-cloud. The bump shows up in all 4 form factors at $Q^2 \simeq 0.25$, and is seen most clearly in G_E^n and in fig. 6 as the red online dashed line. This feature also shows up in the densities determined by Kelly in ref. [59].

Reinforcing this view this is a recent calculation within a chiral quark model by the Tuebingen group [60] that treats the baryons as bound states of constituent quarks, dressed by a cloud of mesons and which gives an excellent description of all four of the electromagnetic form factors.

5 The G_E^p/G_M^p discrepancy and two-photon effects

The recoil polarization measurements of the form factor ratio $\mu_p G_E^p/G_M^p$ contradict the Rosenbluth measurements and it has been suggested that the earlier experiments might have underestimated systematic errors or suffer from normalization problems. The Rosenbluth measurements have been re-examined [61]. This global reanalysis could find no systematic or normalization problems that could account for the discrepancy and concluded that a 5–6% linear ϵ-dependence correction (of origin yet unknown) to the cross-section measurements is required to explain the difference. Several investigators [62–65] have explored the possibility of two-photon exchange corrections (which would be less important in the direct ratio

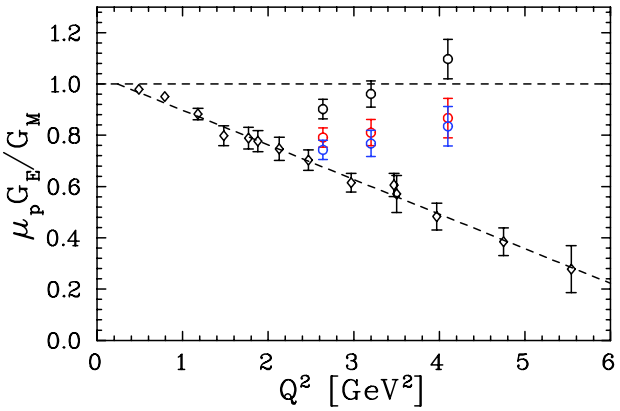

Fig. 7. Corrections to the three data points from the super Rosenbluth data set move those data towards (*i.e.* reduce the value of the form factor ratio) the recoil polarization data set shown with fit (dashed line). Starting with the largest value at each Q^2 is the measured ratio, the ratio with the two-photon corrections of ref. [65] applied and the ratio with the two-photon and with Coulomb corrections [66] applied [67].

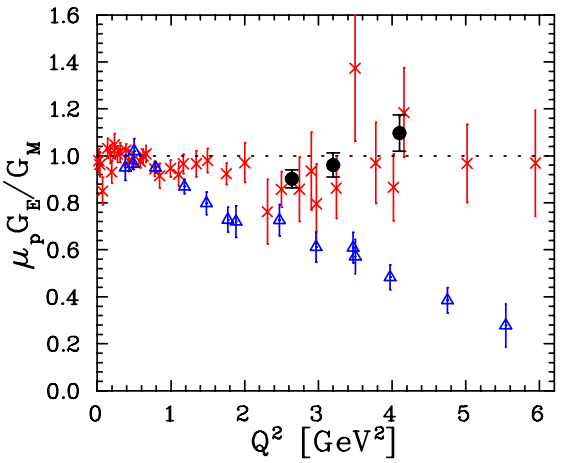

Fig. 8. (Color online) Proton form factor ratio where the (blue) triangles are from recoil polarization [24,26], (red) crosses from the reanalysis of the world's Rosenbluth data set [61] and the filled circles from the recent super Rosenbluth experiment [69].

measurement of recoil polarization) to explain the discrepancy. While only incomplete calculations exist, the results of refs. [62,65] account for part of the difference.

The most recent work by Chen *et al.* [65] employed a different approach than that of ref. [62] in that they describe the process in terms of hard scattering from a quark and use GPDs to describe the quark emission and absorption. They argue that when taking the recoil polarization form factors as input, the addition of the two-photon corrections reproduces the Rosenbluth data. However, Arrington [67] has shown that when the corrections of Chen *et al.* are applied to the new Jefferson Lab Rosenbluth data, which have small errors (see below and fig. 7) only one-half of the discrepancy is explained.

The Rosenbluth-polarization transfer discrepancy has been recently confirmed by a "super" Rosenbluth measurement [68] at Jefferson Lab that was designed to minimize the systematic errors that handicap Rosenbluth measurements. This was achieved by detecting the proton rather than the electron in elastic kinematics. In doing so many of the extreme rate variations and cross-section sensitivities that are normally encountered were avoided. The results [69] show that the discrepancy still exists. See fig. 8.

Direct tests for the existence of two-photon exchange include measurements of the ratio $\frac{\sigma(e^+p)}{\sigma(e^-p)}$, where the real part of the two-photon exchange amplitude leads to an enhancement, and in Rosenbluth data where it can lead to non-linearities in ϵ. There is no experimental evidence of non-linearities in the Rosenbluth data and the e^+/e^- ratio data [70] are of only modest precision, making it difficult to absolutely confirm the presence of two-photon effects in these processes.

It is the imaginary part of the two-photon amplitude that can lead to single-spin asymmetries but again the existing data [71,72] are of insufficient precision to allow one to make a statement. There is, however, one observable that has provided unambiguous evidence for a two-photon effect in ep elastic scattering. Groups in both the US [73] and Europe [74] have measured the transverse polarized beam asymmetry. These measurements are significant but have limited utility in solving the G_E^p discrepancy. The reader interested in more detail about the existence of two-photon effects and their role on the form factor measurements should refer to ref. [67].

Fortunately experiments are planned at Jefferson Lab to look for non-linearities in the Rosenbluth data, for the presence of induced recoil polarization and for an enhancement in the e^+/e^- ratio. We can expect that a concentrated effort in both experiment and theory will reveal the full extent of two-photon effects in the not too distant future.

6 Outlook

A recently completed experiment [75] at Jefferson Lab using a polarized ^{3}He target will provide data on G_E^n out to 3.5 (GeV/c)^2. Next year, the recoil technique will extend the measurement [76] of G_E^p/G_M^p out to 9 (GeV/c)^2. With the 12 GeV upgrade and improvements in targets and recoil polarimeters it anticipated that these quantities can be measured out to 8 and 12 (GeV/c)^2, respectively. Similarly data on G_M^n as high as 14 (GeV/c)^2 can be measured in the upgraded CLAS.

The capabilities of high duty factor accelerators, polarized beams and targets, and polarimeters have produced precision data out to large momentum transfer on the proton and neutron form factors. These new data, and that which will be earned in the next generation of experiments will continue to challenge our view of the structure of the proton and neutron and provide rigorous tests for any QCD-inspired model of nucleon structure.

References

1. S. Galster *et al.*, Nucl. Phys. B **32**, 221 (1971).
2. L. Andivahis *et al.*, Phys. Rev. D **50**, 5491 (1994).
3. P. Bosted, Phys. Rev. C **51**, 409 (1995); E.J. Brash, A. Kozlov, S. Li, G.M. Huber, Phys. Rev. C **65**, 05100 (2002); J.J. Kelly, Phys. Rev. C **70**, 068202 (2004); V.V. Ezhela, B.V. Polishchuk, IHEP 99-48, arXiv:hep-ph/9912401, 1999.
4. W. Brooks, M. Vineyard, Jefferson Lab Experiment E94-107.
5. W. Brooks, J.D. Lachniet, these proceeedings.
6. J.D. Lachniet, PhD Thesis, Carnegie Mellon University, 2005, unpublished UMI-31-86035.
7. A. Lung *et al.*, Phys. Rev. Lett. **70**, 718 (1993).
8. H. Anklin *et al.*, Phys. Lett. B **336**, 313 (1994).
9. E.E.W. Bruins *et al.*, Phys. Rev. Lett. **75**, 21 (1995).
10. H. Anklin *et al.*, Phys. Lett. B **428**, 248 (1998).
11. G. Kubon, H. Anklin *et al.*, Phys. Lett. B **524**, 26 (2002).
12. P. Markowitz *et al.*, Phys. Rev. C **48**, R5 (1993).
13. W. Xu *et al.*, Phys. Rev. Lett. **85**, 2900 (2000).
14. W. Xu *et al.*, Phys. Rev. C **67**, 012201 (2003).
15. N. Meitanis, PhD Thesis, MIT, March 2006, unpublished.
16. S. Platchkov *et al.*, Nucl. Phys. A **510**, 740 (1990).
17. N. Dombey, Rev. Mod. Phys. **41**, 236 (1969).
18. T.W. Donnelly, A.S. Raskin, Ann. Phys. (N.Y.) **169**, 247 (1986); **191**, 81 (1989).
19. A.I. Akhiezer, M.P. Rekalo, Sov. J. Part. Nucl. **3**, 277 (1974).
20. R.G. Arnold, C. Carlson, F. Gross, Phys. Rev. C **23**, 363 (1981).
21. H. Arenhövel, Phys. Lett. B **199**, 13 (1987).
22. H. Arenhövel, W. Leidemann, E.L. Tomusiak, Z. Phys A **331**, 123 (1988); **334**, 363 (1989)(E), Phys. Rev. C **46**, 455 (1992).
23. J. Golak *et al.*, Phys. Rev. C **63**, 034006 (2001); S. Ishikawa, J. Golak *et al.*, Phys. Rev. C **57**, 39 (1998).
24. M.K. Jones *et al.*, Phys. Rev. Lett. **84**, 1398 (2000).
25. O. Gayou *et al.*, Phys. Rev. C **64**, 038292 (2001).
26. O. Gayou *et al.*, Phys. Rev. Lett. **88**, 092301 (2002).
27. T. Eden *et al.*, Phys. Rev. C **50**, R1749 (1994).
28. C. Herberg *et al.*, Eur. Phys. J. A **5**, 131 (1999).
29. M. Ostrick *et al.*, Phys. Rev. Lett. **83**, 276 (1999).
30. R. Madey *et al.* Phys. Rev. Lett. **91**, 122002 (2003).
31. S. Boffi, L.Ya. Glozman, W. Klink, W. Plessas, M. Radici, R.F. Wagenbrunn, Eur. Phys. J. A **14**, 17 (2002).
32. E. Pace, G. Salme, F. Cardarelli, S. Simula, Nucl. Phys. A **666**, 33 (2000).
33. M.R. Frank, B.K. Jennings, G.A. Miller, Phys. Rev. C **54**, 920 (1996).
34. E.L. Lomon, Phys. Rev. C **66**, 045501 (2002).
35. S.J. Brodsky, arXiv:hep-ph/0208158, SLAC-PUB-9281.
36. G. Holzwarth, hep-ph/0201138; Z. Phys. A **356**, 339 (1996) (Fit B2 is shown for the neutron).
37. R. Schiavilla, I. Sick, Phys. Rev. C **64**, 041002 (2001).
38. H. Zhu *et al.*, Phys. Rev. Lett. **87**, 081801 (2001).
39. J. Golak *et al.*, Phys. Rev. C **63**, 034006 (2001).
40. I. Passchier *et al.*, Phys. Rev. Lett. **82**, 4988 (1999).
41. J. Bermuth *et al.*, Phys Lett. B. **564**, 199 (2003); D. Rohe *et al.*, Phys. Rev. Lett. **83**, 4257 (1999).
42. D.I. Glazier *et al.*, arXiv:nucl-ex/0410026.
43. G. Warren *et al.*, Phys. Rev. Lett. **92**, 042301 (2004).
44. V. Ziskin, PhD Thesis, MIT, 2005, unpublished.
45. J. Friedrich, T. Walcher, Eur. Phys. J. A **17**, 607 (2003) (arXiv:hep-ph/0303054).
46. S. Brodsky, G. Farrar, Phys. Rev. D **11**, 1309 (1975); G. Lepage, S. Brodsky, Phys. Rev. D **22**, 2157 (1980); Phys. Scr. **23**, 945 (1981).
47. A.V. Belitsky, X. Ji, F. Yuan, Phys. Rev. Lett. **91**, 092003 (2003).
48. J.P. Ralston, P. Jain, *Proceedings of Workshop on Testing QCD through Spin Observables in Nuclear Targets* (World Scientific, 2003) arXiv:hep-ph/0207129.
49. V. Punjabi, C.F. Perdrisat *et al.*, nucl-ex/0307001; V. Punjabi *et al.*, Phys. Rev. C **71**, 055202 (2005); **71**, 069902 (2005)(E) (arXiv:nucl-ex/0501018).
50. M. Meyerhoff *et al.*, Phys. Lett. B **327**, 201 (1994).
51. J. Becker *et al.*, Eur. Phys. J. A **6**, 329 (1999).
52. H. Gao *et al.*, Phys. Rev. C **50**, R546 (1994).
53. F. Cardarelli, S. Simula, Phys. Rev. C **62**, 065201 (2000); Phys. Lett. B **467**, 1 (1999).
54. G.A. Miller, Phys. Rev. C **66**, 032201(R) (2002).
55. H.W. Hammer, U.G. Meissner, Eur. Phys. J. A **20**, 469 (2004).
56. S. Kopecki *et al.*, Phys. Rev. Lett. **74**, 2427 (1995).
57. M.M. Kaskulov, P. Grabmayr, Eur. Phys. J. A **19**, 157 (2004) (arXiv:nucl-th/0308015).
58. G.A. Miller, Phys. Rev. C **66**, 032201 (2002) (arXiv:nucl-th/0207007).
59. J.J. Kelly, Phys. Rev. C **66**, 065203 (2002) (arXiv:hep-ph/0204239); AIP Conf. Proc. **698**, 393 (2004).
60. A. Faessler, T. Gutsche, V.E. Lyubovitskij, K. Pumsa-ard, Phys. Rev. D **73**, 114021 (2006) (arXiv:hep-ph/0511319).
61. J. Arrington, Phys. Rev. C **68**, 034325 (2003).
62. P.G. Blunden, W. Melnitchouk, J.A. Tjon, Phys. Rev. Lett. **91**, 142304 (2003).
63. M.P. Rekalo, E. Tomasi-Gustafsson, Eur. Phys. J. A **22**, 331 (2004).
64. P.A.M. Guichon, M. Vanderhaeghen, Phys. Rev. Lett. **91**, 142303 (2003).
65. Y.C. Chen, A. Afanasev, S.J. Brodsky, C.E. Carlson, M. Vanderhaeghen, Phys. Rev. Lett. **93**, 122301 (2004).
66. J. Arrington, I. Sick, Phys. Rev. C **70**, 028203 (2004).
67. J. Arrington, Phys. Rev. C **71**, 015202 (2005) (arXiv:hep-ph/0408261).
68. J. Arrington, R. Segel, Jefferson Lab Experiment E01-001.
69. I.A. Qattan *et al.*, Phys. Rev. Lett. **94**, 142301 (2005) (arXiv:nucl-ex/0410010).
70. J. Mar *et al.*, Phys. Rev. Lett. **21**, 482 (1968).
71. H.C. Kirkman *et al.*, Phys. Lett. B **32**, 519 (1970).
72. T. Powell *et al.*, Phys. Rev. Lett. **24**, 753 (1970).
73. SAMPLE Collaboration (S.P. Wells *et al.*), Phys. Rev. C **63**, 064001 (2001).
74. F.E. Maas *et al.*, Phys. Rev. Lett. **94**, 082001 (2005) (arXiv:nucl-ex/0410013).
75. B. Wojtsekhowski, G. Cates, spokespersons, Jefferson Lab Proposal PR02-013.
76. E. Brash, M. Jones, C. Perdrisat, V. Punjabi, spokespersons, Jefferson Lab Proposal PR04-108.